Polymer immiscibility enhanced by thermal fluctuations toward crystalline order

Yu Ma,[1] Wenbing Hu,[1,*] and Howard Wang[2,†]

[1]*Department of Polymer Science and Engineering, School of Chemistry and Chemical Engineering, State Key Laboratory of Coordination Chemistry, Nanjing University, 210093 Nanjing, China*

[2]*Department of Mechanical Engineering, Binghamton University, Binghamton, New York 13902, USA*

We report dynamic Monte Carlo simulations of binary polymer blends. The blends exhibit liquid-liquid phase separation influenced by the nearby crystallization of one component. We found that both binodal and spinodal boundaries of liquid-liquid phase separation shift up above the predictions of the mean-field lattice theory. The enhancement of immiscibility can be assigned to the thermal fluctuations toward better parallel order of the crystallizable chains in the blends, which has been neglected in the mean-field theory. This result serves as a theoretical background to explain the related experimental observations.

I. INTRODUCTION

Blending has been widely applied in achieving desirable properties of polymeric materials at a reduced cost. Partially miscible binary polymer blends typically exhibit upper critical solution temperatures (UCST), below which homogeneous mixtures become unstable and the liquid-liquid phase separation (LLPS) occurs. Among the theories describing LLPS of polymer blends, Flory-Huggins lattice theory has been accepted as being of fundamental importance on account of its simplicity with less expense of accuracy [1–4]. According to this theory, the locations of UCST are dominated by the balance between the enthalpy source from the exchange interactions of two species (described by an interaction parameter B) and the mixing entropy scaled inversely with the polymer chain length of each component. On the other hand, polymer blends are often used in semicrystalline states as a result of crystallization, also known as liquid-solid phase transition (LSPT). Understanding the interplay between LSPT and LLPS is of significant technological importance to the morphological control in the processing of polymer blends and therefore, deserves further investigation.

Recently, it has been found that the molecular driving forces for polymer crystallization can be described by an anisotropic interaction parameter denoted as E_p, provided that the parameter measures the energy favoring the parallel packing of two neighboring bonds of lattice polymers [5]. By employing both the interaction parameters B and E_p, the mean-field lattice theory can calculate the phase diagrams of LLPS and LSPT in polymer solutions [6] as well as in polymer blends [7]. One achievement of this approach is that under athermal mixing of polymer blends ($B=0$), the component-selective crystallizability ($E_p \neq 0$) still gives rise to LLPS, explaining the partial immiscibility in the tacticity mixtures of several common polymers [7].

In the experiments, recent work by Wang and co-workers have identified several polyolefin blends exhibiting the interplay of LLPS and LSPT, where the observed UCST could be either above the equilibrium melting temperature, T_m^0 [8,9], or below it [10], subject to the chosen component species. In the latter case, a discrepancy between UCST as measured by optical microscopy and as extrapolated from small-angle neutron-scattering data with a mean-field assumption has been observed [10], indicating an enhanced immiscibility probably due to the potentiality of crystallization in the metastable liquid.

Up to now, it has not been well evidenced that thermal fluctuations for the crystallization from the liquid can enhance the immiscibility of polymer blends. The main purpose of our present work is to address the issue raised here, by a direct comparison between the predictions calculated from the mean-field theory and the results collected from the corresponding molecular simulations, on the simple basis that the former neglects the thermal fluctuations and the latter carries them.

In this paper, we use dynamic Monte Carlo simulations to illustrate the phase diagrams of LLPS of lattice polymer blends approaching to LSPT from high temperatures. It will be shown that strong thermal fluctuations for parallel ordering of crystallizable chains in the vicinity of LSPT indeed enhance LLPS by shifting up UCST beyond the predictions of the mean-field theory.

The paper is organized as follows. After the introduction section, two approaches of phase diagrams from the mean-field lattice theory and from molecular simulations are introduced separately. Then, comparisons of their results will be carried out in company with some discussions. The paper ends with a few concluding remarks.

II. MEAN-FIELD PHASE DIAGRAMS OF POLYMER BLENDS

The statistical thermodynamics of polymer blends have been well described by the classical Flory-Huggins theory [1–4]. There have been many extensions of this theory, such as the equation-of-state theory concerning the compressibility of polymer fluids [11], and the lattice-cluster theory concerning the geometrical details of chain structures [12]. For the sake of simplicity, we followed the classical Flory-Huggins approach to calculate the phase diagrams of LLPS

---

*wbhu@nju.edu.cn

†wangh@binghamton.edu

and LSPT separately [13], and then compared the theoretical results with the data collected from molecular simulations under the parallel conditions.

Assuming that in a regular lattice with the coordination number q, the total volume n consists of two polymer species of uniform chain lengths r and the molecular numbers of n_1 and n_2, respectively, and the first species is noncrystallizable ($E_p = 0$) while the second one is crystallizable ($E_p \neq 0$), the partition function for such a binary polymer blend is thus given by [7]

$$Z = \left(\frac{n}{n_1}\right)^{n_1} \left(\frac{n}{n_2}\right)^{n_2} \left(\frac{q}{2}\right)^{n_1+n_2} z_c^{(n_1+n_2)(r-2)}$$
$$\times e^{-(n_1+n_2)(r-1)} z_p^{n_2(r-1)} z_m^{n_2 r}, \quad (1)$$

where

$$z_c = 1 + (q-2)\exp\left(-\frac{E_c}{kT}\right),$$

$$z_p = \exp\left[-\frac{q-2}{2}\left(1 - \frac{2n_2(r-1)}{qn}\right)\frac{E_p}{kT}\right],$$

$$z_m = \exp\left(-\frac{n_1 r}{n}\frac{(q-2)B}{kT}\right),$$

and one more interaction parameter E_c describes the preference of collinear connection of two consecutive bonds along the chain, which reflects the chain inflexibility [13]. As usual, k is the Boltzmann constant and T the absolute temperature. In Eq. (1), z_m results from a mean-field treatment of the mixing interactions between two species, and z_p results from a similar mean-field treatment of the anisotropic interactions between crystallizable chains, while the others result from the classical lattice statistics for the binary blends of equally semiflexible polymer chains.

The coexistence lines of LSPT can be calculated on the basis of the chemical potentials equivalent between liquid and solid states, as given by

$$\mu^S - \mu^0 = \mu^L - \mu^0, \quad (2)$$

where μ^0 is the chemical potential of polymers at the fully ordered ground state. Since polymers in the solid state bear no large difference of the free energy ΔF from those in the ground state, we have

$$\mu^S - \mu^0 = \frac{\partial \Delta F^S}{\partial n_2} = \frac{\Delta F^S}{n_2} \approx 0. \quad (3)$$

Inserting this result and the partition function of the liquid polymers and solving Eq. (2), one can obtain the equilibrium melting points for variable compositions, which constitute the coexistence line of LSPT.

On the other hand, the binodal lines of LLPS can be calculated on the basis of the chemical potentials equivalent between two coexisting phases with different compositions, labeled with a and b, respectively,

$$\Delta\mu_{1a} = \Delta\mu_{1b},$$

$$\Delta\mu_{2a} = \Delta\mu_{2b}, \quad (4)$$

The mixing free energy per unit volume Δf_{mix} derived from the partition function in Eq. (1) can be used to solve the above parallel equations, as given by [7]

$$\frac{\Delta f_{\text{mix}}}{k_B T} = \frac{\phi_1}{r}\ln\phi_1 + \frac{\phi_2}{r}\ln\phi_2 + \phi_1\phi_2$$
$$\times\left[(q-2)\frac{B}{k_B T} + \left(1 - \frac{2}{q}\right)\left(1 - \frac{1}{r}\right)^2\frac{E_p}{k_B T}\right], \quad (5)$$

where ϕ_1 and ϕ_2 are the volume fractions of two species, respectively. Note that the present expression inherits the format of the classical Flory-Huggins equation, with the interaction parameter containing both B and E_p contributions. Accordingly, the spinodal line of LLPS can be obtained from the second derivative of the mixing free energy to the composition, and the result is given by

$$\frac{1}{\phi_1} + \frac{1}{\phi_2} = 2r\left[(q-2)\frac{B}{k_B T} + \left(1 - \frac{2}{q}\right)\left(1 - \frac{1}{r}\right)^2\frac{E_p}{k_B T}\right]. \quad (6)$$

III. SIMULATION TECHNIQUES

Dynamic Monte Carlo simulations of lattice polymers have been widely applied in the study of microscopic crystallization behaviors of various polymeric systems [13]. The present simulations assumed that polymer chains are moving in 32^3 cubic lattice, via microrelaxation performing single-site jumping of the monomers sometimes with partial sliding diffusion along the chain to hold the bond lengths in the unit of lattice distance (the outreach in each step of microrelaxation). The microrelaxation allows the bonds to stay either along the lattice axes or along the face and body diagonals, and hence the coordination number of the cubic lattice is as high as 26 (six neighbors along lattice axes, 12 along face diagonals, and eight along body diagonals). The conventional periodic boundary conditions were employed to study the bulk polymer systems. To mimic the hard-core volume repulsions of polymers, double occupations and bond crossings are not allowed. A total number of 960 chains, each containing 32 monomers, were placed into the cubic lattices. Some void sites (6.25%) are necessary for the microrelaxation of polymers in the lattice, playing the role as the free volume in the bulk polymer phase although in reality the free volume fraction of bulk polymers may be different or even more. In the binary blend, the species share the total amount of polymer chains according to their compositions. The homogeneous melts were obtained after a long-term microrelaxation of the preset fully ordered chains under athermal conditions (corresponding to the infinitely high temperatures in the sense of statistical thermodynamics).

The homogeneous melts were then slowly cooled down to trace the liquid-liquid demixing induced by a template, like in the previous simulations of polymer solutions [6]. Since on cooling from high temperatures, the primary nucleation in

either LSPT or LLPS requires a significant supercooling, the spontaneous phase transitions usually occur at the temperatures away from the thermodynamic boundary we want to obtain. Introducing a template for phase transitions can effectively avoid the primary nucleation process and thus largely eliminates the supercooling on cooling. The template is a double layer formed by 64 extended chains and oriented along a face diagonal of the cubic box. Therefore, in the molecular simulations employing such a template, the onset temperature of LLPS on cooling could be used to determine the tentative liquid-liquid binodal boundary. On the other hand, since the metastability limit of demixing would eventually approach at the vicinity of the spinodal [14], in the simulation systems without the template, the onset point of spontaneous LLPS on cooling could be treated as the tentative spinodal boundary.

On cooling, the conventional Metropolis sampling was employed and the variation of the potential energy in each step of microrelaxation was given by

$$\Delta E = \frac{bB + pE_p + cE_c}{kT} = \left(b\frac{B}{E_c} + p\frac{E_p}{E_c} + c \right) \frac{E_c}{kT}, \qquad (7)$$

where b, p, and c were the net amounts of mixing pairs, nonparallel-bond pairs, and noncollinear connections of bonds along the chain, corresponding to the associated energy parameters. In practice, the system underwent the stepwise cooling from $T = 35E_c/k$ to a value close to zero, with a step length 0.02 and a step period of 300 Monte Carlo cycles (MCCs). One MCC is defined as the amount of trial moves equivalent to the number of monomers in the sample system. This cooling process is relatively slow in the time window of our observation, and affects the speed of the growing process after the initiation of phase transitions. But the onset of phase transition will be less affected. Here, for the sake of simplicity, we temporarily neglected the effect of cooling rates to the onset of phase transitions.

To monitor the LSPT on cooling, the degree of crystallinity was defined as the fraction of crystallizable bonds containing more than five parallel neighbors of the same component. Meanwhile, to monitor the LLPS on cooling, the demixing parameter was defined as the fraction of noncrystallizable monomers surrounded with more than five other noncrystallizable monomers. In principle, the parallel and the monomer neighbors may change their numbers from zero to 24 (two consecutive neighbors along the chain are subtracted from the coordination number 26 of the cubic lattice). The demarcation criteria for new phases were deliberately chosen at five, in order to allow the parallel order and the condensed phases to include those bonds and/or monomers located at the interfaces. The reported observations were averaged over the last 200 MCCs at each step of the cooling process. A typical result for such a cooling process is shown in Fig. 1, where the onset temperature of LLPS was obtained at the crossover of two extrapolations from the transition region and from the mixing region, respectively.

Figure 2 demonstrates that LLPS induced by a template occurs at the temperature much higher than that without a template on the cooling process, hence the template effec-
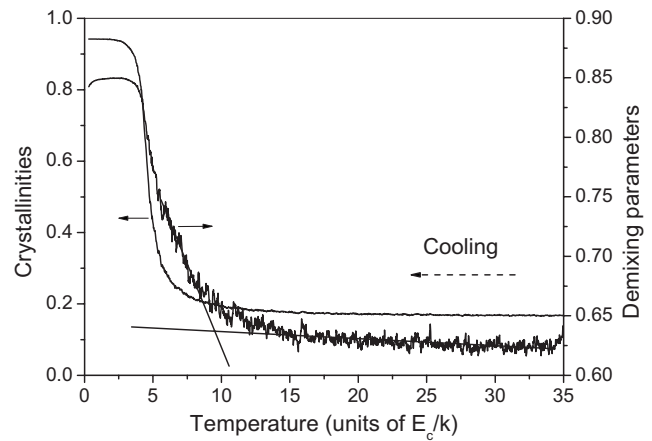

FIG. 1. Cooling curves of crystallinities (left-hand axis) and demixing parameters (right-hand axis) of the symmetric polymer blend with a volume fraction of the crystallizable species $\phi_2 = 0.4$, $E_p/E_c = 1$, and $B/E_c = -0.02$, obtained from the simulations of sample systems containing a template. Two arrows are indicating the corresponding axes. The crossover of two extrapolations defines the onset of LLPS.

tively eliminates the supercooling required for the initiation of phase transitions.

It is well known that the approaches of simulations at the boundaries of phase transitions exhibit the finite-size effect [15]. We have examined the finite-size effect of cubic lattice boxes on LLPS through performing otherwise identical simulations with boxes of various sizes up to 64^3, as shown in Fig. 3. Figure 3 demonstrates that at the chosen composition nearby to the critical point, the onset temperatures become less sensitive to the linear size of the box when the latter increases up to 32. Therefore, the finite-size effect can be tentatively disregarded in the simulation results obtained from the 32^3 boxes, especially when a template coexists in the sample systems and a long-range correlation is not a prerequisite of the initiation of phase transitions.
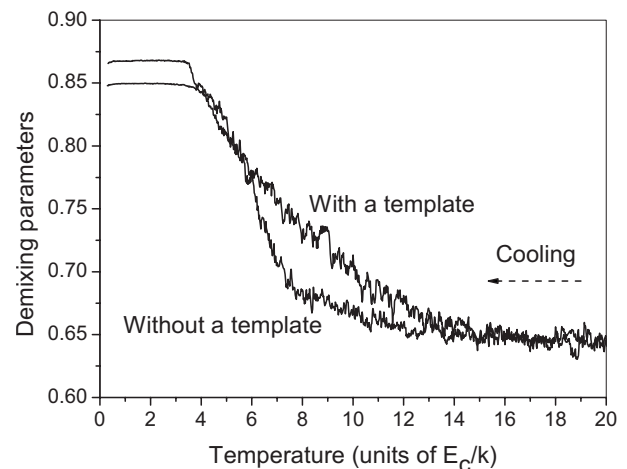

FIG. 2. Cooling curves of demixing parameters of a symmetric polymer blend with $\phi_2 = 0.4$, $E_p/E_c = 1$, and $B/E_c = 0$, obtained from the simulations of the sample systems with or without a template.
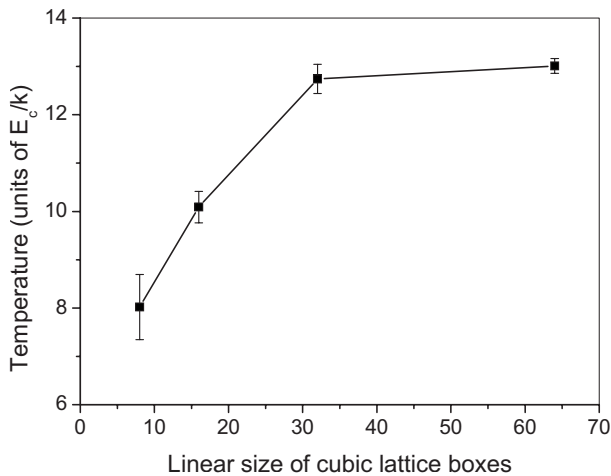
FIG. 3. Onset temperatures of LLPS for symmetric polymer blends with $\phi_2=0.4$, $E_p/E_c=1$, and $B/E_c=0$, obtained from the simulations using various sizes of cubic lattice boxes without a template for phase transitions. The reported data are averaged over five individual simulation results (different seeds for random-number generation). The segments are drawn to guide the eyes.

IV. RESULTS AND DISCUSSION

Polymer blends were designed to exhibit the interplay of LLPS and LSPT. To this end, the bonds of the crystallizable species had a value of E_p/E_c fixed at 1, while the reduced energy parameters B/E_c were variable to adjust UCST approaching LSPT boundaries from high temperatures. Figure 4 shows that the theoretical binodals of LLPS (the solid curves) are sensitive to the variable B/E_c, but LSPT coexistence lines (the dashed curves) are not. This result reflects the fact that B/E_c dominates LLPS and E_p/E_c dominates LSPT.
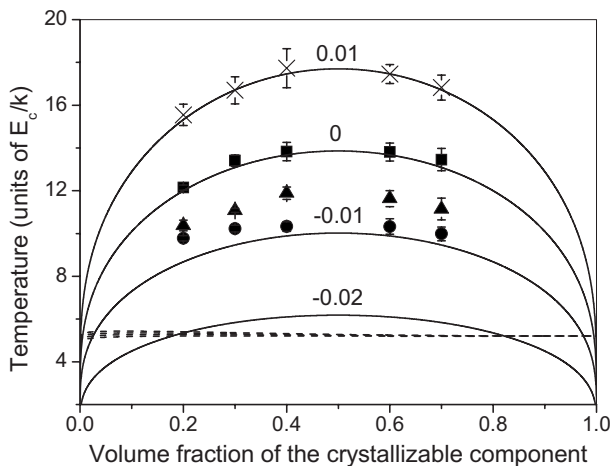

FIG. 4. LLPS binodals (solid curves) and LSPT lines (dashed curves) of symmetric polymer blends with one component crystallizable ($E_p/E_c=1$) and variable B/E_c values as denoted nearby to the solid curves, predicted by the mean-field lattice theory. The data points ($B/E_c=0.01$ crosses, 0 squares, -0.01 triangles, and -0.02 spheres) are "real" binodals obtained from simulations of lattice polymer blends with a template. Each data point was averaged over five individual simulation results.
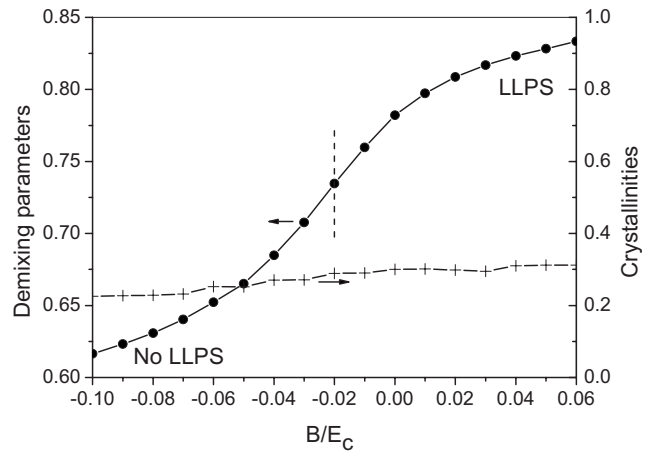

FIG. 5. Demixing parameters (spheres, left-hand axis) and crystallinities (crosses, right-hand axis) obtained from the simulations of symmetric polymer blends with $\phi_2=0.4$, $E_p/E_c=1$, and varying B/E_c values at $T=6E_c/k$. Each data of demixing parameters was averaged over 10^4 samples collected with 10 MCC intervals during annealing, while each data for crystallinities was obtained at the end of annealing. Two short arrows indicate the corresponding axes. The dashed line marks the boundary of the two mixing status. The segments are drawn to guide the eyes.

Figure 4 compares the simulation binodals of LLPS (symbols) with the theoretical predictions (curves). They appear in good agreement when the binodals are far above LSPT boundaries; however, when the binodals are close to LSPT boundaries, simulation binodals significantly shift up to the temperatures higher than the corresponding theoretical curves, indicating an enhanced immiscibility of polymers in the vicinity of LSPT.

The component-selective crystallization manifests itself as a behavior of demixing. To make sure that the enhanced immiscibility is not induced by the early stage of crystallization on cooling but rather, by something buried in the liquid phase, we evaluated the mixing status of polymers with variable values of B/E_c, at a fixed temperature $T=6.0E_c/k$ just above LSPT boundaries (see Fig. 4), as well as at a fixed concentration $\phi_2=0.4$. Homogeneous blends were slowly cooled down from $T=25$ to $6E_c/k$ with a step length 0.02 and a step period 200 MCCs, and then isothermally annealed at $6E_c/k$ for 10^5 MCCs for the sample systems containing a template. After a long-term annealing under the above conditions, both the demixing parameters and the crystallinities were calculated. The results are shown in Fig. 5.

Figure 5 demonstrates that the crystallinities do not show any crystallization in all the concerned B/E_c values, but exhibit the slightly enhanced fluctuations towards the parallel order of crystallizable chains along with the enhanced LLPS. On the other hand, the demixing parameters reveal two extremities of mixing status, corresponding to LLPS and no LLPS, respectively. In the case of $B/E_c=-0.02$, the demixing parameter is stable at the middle of the phase separation. If the demixing was induced by a saturate crystallization, the demixing parameter could not be stable at the middle value. Therefore, in the case of $B/E_c=-0.02$, the demixing on cooling can still be regarded as an intrinsic LLPS rather than
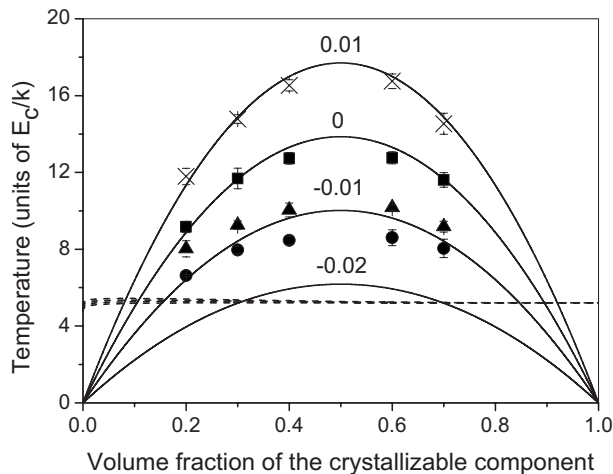
FIG. 6. LLPS spinodals (solid lines) and LSPT curves (dashed lines) of the symmetric polymer blends with one component crystallizable ($E_p/E_c=1$) and variable B/E_c values as denoted nearby to the solid curves, predicted by the mean-field theory. Data points ($B/E_c=0.01$, crosses; 0, squares; −0.01, triangles; and −0.02, spheres) were collected through the simulations of lattice polymer blends without a template for phase separation, and each data was averaged over five individual simulation results.

LSPT, although the onset point of demixing has shifted up far above the theoretical LLPS binodals.

Similarly, the theoretical predictions and the simulation results of LLPS spinodals were also compared in Fig. 6, where the significant shifts occur again in the vicinity of LSPT boundaries. This result is consistent with the binodals and implies that the introduced template has no responsibility to the observed shift up of binodals.

In the case of $B/E_c=-0.01$, simulation spinodals shown in Fig. 6 seem to fit better for the theoretical predictions than the corresponding binodals shown in Fig. 4. This better fitting could be attributed to the shifting back of spinodals due to the finite-size effect in simulations, if we consider the fact that the finite-size effect becomes relatively significant in the samples containing no template.

As mentioned in the introduction section, the rational to explain the enhancement of polymer immiscibility in the vicinity of the solidification lines can be assigned to the strong thermal fluctuations of anisotropic interactions (i.e., E_p energies), which are responsible for LSPT of the crystallizable component at low temperatures. The applied parallel attractions between crystallizable bonds are actually similar with the Maier-Saupe interactions responsible for the thermotropic isotropic-nematic (*I-N*) liquid-crystal phase transition [16]. At the temperatures above the equilibrium *I-N* transition, the pretransitional effect induced by the ordering fluctuations has been discussed under the scheme of the Landau theory for phase transitions [17,18]. The correlation length of the orientational order diverges as the critical temperature is approached, which reflects the metastability limit of the disordered state [19]. The crossover from the mean-field region to the critical region (namely the Ginzburg criteria [20]) also exists in such fluctuations of parallel ordering. Concerning the demixing aspect of the ordering process, the size of the
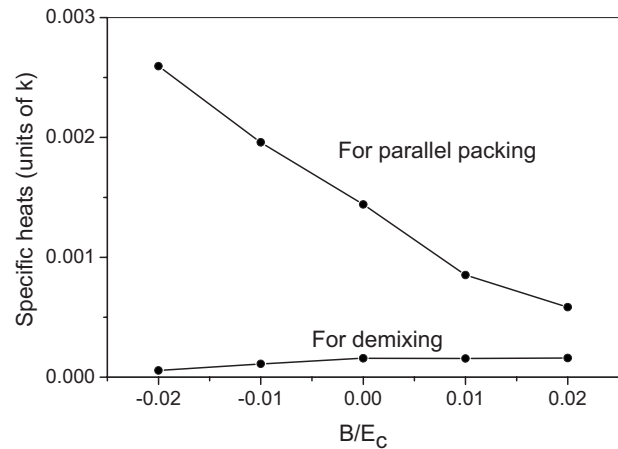
critical region may scale inversely with the chain length, like in the case of LLPS [21]. Indeed, in the previous molecular simulations of statistical copolymers, we have observed a small degree of crystallinity generated by the thermal fluctuations in the metastable liquid before crystallization, which increases with the decrease of temperatures as well as the decrease of the content of noncrystallizable comonomers [22].

The extent of thermal fluctuations is usually characterized by the specific heat. Therefore, we calculated the specific heats sourced from the parallel packing and from the demixing, respectively. The specific heat of parallel packing is given by

$$\frac{C_V(\text{parallel})}{k} = \frac{\langle E^2 \rangle - \langle E \rangle^2}{4} \left(\frac{E_c}{kT}\right)^2 \left(\frac{E_p}{E_c}\right)^2, \quad (8)$$

where E is the number of crystallizable bonds parallel around each crystallizable bond, and $\langle \cdots \rangle$ is an ensemble average. The specific heat of demixing is given by

$$\frac{C_V(\text{demixing})}{k} = (\langle M^2 \rangle - \langle M \rangle^2) \left(\frac{E_c}{kT}\right)^2$$
$$\times \left[\frac{B}{E_c} + \frac{1}{q}\left(1 - \frac{1}{r}\right)^2 \frac{E_p}{E_c}\right]^2, \quad (9)$$

where M is the number of crystallizable monomers around each crystallizable monomer. In Eq. (9), we made use of the mean-field treatment to the demixing energy in Eq. (5), for each pair of monomer-solvent contacts whose number is equal to one-half of the monomer-monomer contacts. The results are shown in Fig. 7 for the samples containing no template annealed at the fixed concentration $\phi_2=0.4$ and the fixed energy parameter $E_p/E_c=1$, under variable temperatures $T=10.33$, 11.89, 13.82, 17.73, and 21.25 E_c/k, corresponding to the cases of $B/E_c=-0.02$, −0.01, 0, 0.01, and 0.02, respectively. The above temperatures are the onsets of

FIG. 7. Specific heats of parallel packing and demixing as denoted nearby for the samples with the variable B/E_c at the corresponding temperatures 10.33, 11.89, 13.82, 17.73, and 21.25 E_c/k, respectively, and with the fixed concentration $\phi_2=0.4$ and the fixed energy parameter $E_p/E_c=1$. The segments are drawn to guide the eyes.

demixing reported in Fig. 4. At these temperatures, the bulk thermal fluctuations of demixing are going to generate the thermodynamic phase separation with the help of the preset template. The data were collected during the period of 2 $\times 10^5$ MCCs with 200 MCC intervals to calculate the specific heats.

In Fig. 7, one can see that the specific heats of parallel packing significantly increase with the decrease of B/E_c, while the specific heats of demixing have been little affected because they are all coordinated at the onset temperatures of demixing corresponding to the variable B/E_c values. This observation evidences our above rational that with the decrease of temperatures, the thermal fluctuations of parallel packing contribute more and more to the thermal fluctuations of demixing, eventually causing the shifting-up of both binodals and spinodals above the predictions of the mean-field lattice theory.

In the mean-field lattice theory, crystallizable bonds are assumed to distribute homogeneously and to orient randomly. However, when the temperature approaches down to the melting point, strong thermal fluctuations due mainly to the anisotropic interactions yield more parallel packing of crystallizable bonds, and thus enhance the inhomogeneous distribution of the crystallizable component. The current mean-field lattice theory neglects these anisotropic fluctuations, and therefore underestimates the actual contribution of E_p in the mixing free energy described in Eq. (5). In consequence, the simulation results of UCST shift up above the theoretical predictions.

Recently, Schwahn has written a review on the crossover behaviors of LLPS from the critical to mean-field regions [23]. According to this review, the Flory-Huggins interaction parameters and the phase boundaries must precisely determined with the more serious consideration to the composition fluctuations. In this sense, the shifting-up of UCST can be regarded as the consequence of a coupling between the composition fluctuations and the fluctuations towards the crystalline order in the vicinity of the solidification lines. Since the critical regions for both fluctuations scale inversely with the polymer chain length, and the applied chain lengths in our simulations are relatively small, the coupling effect appears quite significant here. In reality, however, when the polymer chains in the blends are quite long, the critical regions and their coupling are expected to occur in a much narrower temperature range. This coupling effect in the critical behaviors of polymer phase transitions demands further investigations.

V. CONCLUDING REMARKS

By means of dynamic Monte Carlo simulations and the mean-field lattice theory, we have investigated the liquid-liquid phase separation of polymer blends influenced by the nearby crystallization of one component. The results revealed that the immiscibility of blends could be enhanced by thermal fluctuations of anisotropic interactions that are responsible for the crystallization at low temperatures. This enhancement implies the composition fluctuations coupling with the fluctuations towards crystalline order. The present observation evidences a theoretical background that can be applied to explain the related experimental observations on real polymers.

In a broad sense, our present observation casts new insights into a better description of polymer phase transitions. Further, attention has been called to the role of thermal fluctuations toward crystalline order in the critical behaviors of liquid-liquid phase separations.

[1] P. J. Flory, J. Chem. Phys. **10**, 51 (1942).

[2] M. L. Huggins, Ann. N.Y. Acad. Sci. **43**, 1 (1942).

[3] R. L. Scott, J. Chem. Phys. **17**, 279 (1949).

[4] H. Tompa, Trans. Faraday Soc. **45**, 1142 (1949).

[5] W.-B. Hu, J. Chem. Phys. **113**, 3901 (2000).

[6] W.-B. Hu, V. B. F. Mathot, and D. Frenkel, J. Chem. Phys. **118**, 10343 (2003).

[7] W.-B. Hu and V. B. F. Mathot, J. Chem. Phys. **119**, 10953 (2003).

[8] H. Wang, K. Shimizu, E. K. Hobbie, Z. G. Wang, J. C. Meredith, A. Karim, E. J. Amis, B. S. Hsiao, E. T. Hsieh, and C. C. Han, Macromolecules **35**, 1072 (2002).

[9] G. Matsuba, K. Shimizu, H. Wang, Z. G. Wang, and C. C. Han, Polymer **44**, 7459 (2003).

[10] H. Wang (unpublished).

[11] For a good review, see I. C. Sanchez and M. T. Stone, in *Polymer Blends: Formulation and Performance*, edited by D. R. Paul and C. B. Bucknall (Wiley, New York, 2000), Vol. 1, Chap. 2.

[12] K. F. Freed and J. Dudowicz, Adv. Polym. Sci. **183**, 63 (2005).

[13] W.-B. Hu and D. Frenkel, Adv. Polym. Sci. **191**, 1 (2005).

[14] Z. G. Wang, J. Chem. Phys. **117**, 481 (2002).

[15] D. P. Landau and K. Binder, *A Guide to Monte Carlo Simulations in Statistical Physics* (Cambridge University Press, Cambridge, 2000), Chap. 5.

[16] W. Maier and A. Y. Saupe, Z. Naturforsch. A **14A**, 882 (1959); **15A**, 287 (1960).

[17] P. G. de Gennes, Phys. Lett. **30A**, 454 (1969).

[18] C.-P. Fan and M. J. Stephen, Phys. Rev. Lett. **25**, 500 (1970).

[19] P. G. de Gennes, *The Physics of Liquid Crystals* (Oxford University Press, Oxford, 1975), Chap. 2.

[20] L. P. Kadanoff, *Statistical Physics: Statics, Dynamics and Renormalization* (World Scientific, Singapore, 2000), Chap. 11.

[21] P. G. de Gennes, *Scaling Concepts in Polymer Physics* (Cornell University Press, Ithaca, NY, 1979), Chap. 4.

[22] W.-B. Hu, V. B. F. Mathot, and D. Frenkel, Macromolecules **36**, 2165 (2003).

[23] D. Schwahn, Adv. Polym. Sci. **183**, 1 (2005).